J. theor. Biol. (2000) **210,** 167–186
doi:10.1006/jtbi.2000.2294, available online at http://www.idealibrary.com on IDEAL®

A Model for a Network of Phosphorylation–dephosphorylation Cycles Displaying the Dynamics of Dominoes and Clocks

DIDIER GONZE AND ALBERT GOLDBETER†

Faculté des Sciences, Université Libre de Bruxelles, Campus Plaine, C.P. 231, *B*-1050 *Brussels, Belgium*

(*Received on* 20 *June* 2000, *Accepted in revised form on* 28 *November* 2000)

We consider a model for a network of phosphorylation–dephosphorylation cycles coupled through forward and backward regulatory interactions, such that a protein phosphorylated in a given cycle activates the phosphorylation of a protein by a kinase in the next cycle as well as the dephosphorylation of a protein by a phosphatase in a preceding cycle. The network is cyclically organized in such a way that the protein phosphorylated in the last cycle activates the kinase in the first cycle. We study the dynamics of the network in the presence of both forward and backward coupling, in conditions where a threshold exists in each cycle in the amount of protein phosphorylated as a function of the ratio of kinase to phosphatase maximum rates. We show that this system can display sustained (limit-cycle) oscillations in which each cycle in the pathway is successively turned on and off, in a sequence resembling the fall of a series of dominoes. The model thus provides an example of a biochemical system displaying the dynamics of dominoes and clocks (Murray & Kirschner, 1989). It also shows that a continuum of clock waveforms exists of which the fall of dominoes represents a limit. When the cycles in the network are linked through only forward (positive) coupling, bistability is observed, while in the presence of only backward (negative) coupling, the system can display multistability or oscillations, depending on the number of cycles in the network. Inhibition or activation of any kinase or phosphatase in the network immediately stops the oscillations by bringing the system into a stable steady state; oscillations resume when the initial value of the kinase or phosphatase rate is restored. The progression of the system on the limit cycle can thus be temporarily halted as long as an inhibitor is present, much as when a domino is held in place. These results suggest that the eukaryotic cell cycle, governed by a network of phosphorylation–dephosphorylation reactions in which the negative control of cyclin-dependent kinases plays a prominent role, behaves as a limit-cycle oscillator impeded in the presence of inhibitors. We contrast the case where the sequence of domino-like transitions constitutes the clock with the case where the sequence of transitions is passively coupled to a biochemical oscillator operating as an independent clock.

1. Introduction

A discussion of the dynamics of the cell division cycle led Murray & Kirschner (1989) to publish a seminal paper entitled "Dominoes and clocks: the union of two views of the cell cycle." In this paper, the authors compared the operation of a continuous biochemical oscillator controlling a sequence of biochemical steps with the sequential falling of dominoes in a network of biochemical reactions. The latter view often corresponds to verbal descriptions of chains of biochemical

† Author to whom correspondence should be addressed. E-mail: agoldbet@ulb.ac.be

0022–5193/01/100167 + 20 $35.00/0

events which appear to follow each other sequentially, one step leading to the next after some threshold is passed. When the sequence occurs in a repetitive manner, the system behaves as a clock but the question arises as to whether it still corresponds to a continuous (limit-cycle) oscillator.

The goal of the present paper is to unify the two types of dynamics (dominoes vs. clocks) by means of a theoretical model built specifically for this purpose. Thus, we consider a network of biochemical reactions organized in a cyclical manner, and incorporate thresholds allowing the sequential progression from one step to the next in this network. We investigate the conditions in which such a cyclical network of biochemical reactions operates as a limit-cycle oscillator.

To include thresholds in a simple, straightforward manner, we consider a series of covalent modification (e.g. phosphorylation–dephosphorylation) cycles operating in conditions where the modifying enzymes are saturated by their substrate. Such conditions lead to the phenomenon of *zero-order ultrasensitivity* (Goldbeter & Koshland, 1981, 1982) by which the fraction of protein modified at steady state varies in a sigmoidal manner, characterized by a steep threshold, as the ratio of maximum rates of phosphorylation and dephosphorylation progressively increases.

In the network model, phosphorylation–dephosphorylation cycles are coupled through regulatory interactions and endowed with threshold-like properties. Each phosphorylated protein in the network activates the phosphorylation of the next element (positive, forward regulation) as well as the dephosphorylation of a previous protein in the network (negative, backward regulation). The protein phosphorylated in the last step activates protein phosphorylation in the first step of the network. We show that this hypothetical model can display the dynamics of dominoes and clocks, as well as coexistence between multiple steady states or between an oscillatory regime and a steady state.

In Section 2, we present the abstract model of a cyclically organized network of phosphorylation–dephosphorylation cycles coupled through forward and backward regulatory interactions. The oscillatory behavior of the model is analysed in Section 3. The effect of an inhibitor arresting the oscillations is considered in Section 4. In Section 5, we analyse the dynamics in the presence of only backward or forward coupling between the various phosphorylation–dephosphorylation cycles of the network. We show that in the latter case bistability can occur instead of oscillations, while in the former case either multistability or oscillations are possible, depending on the number of cycles in the network.

The model provides an illustration of a case where the two views of the oscillatory dynamics of a biochemical reaction network can be unified: the system evolves toward a limit cycle (clock) but retains properties of domino-like transitions as the successive phases of the oscillations progressively unfold in a stepwise manner. The addition of a kinase or phosphatase inhibitor directly leads to the arrest of the clock and amounts to holding the dominoes in place; the fall of the dominoes and the oscillations resume as soon as this negative control is removed.

It is important to distinguish the case where the sequence of domino-like transitions itself operates as a clock from the case where the sequence of transitions is passively linked to an independent clock. To clarify the difference between the two situations, we consider in Section 6, for illustrative purposes, a model in which a linear sequence of phosphorylation–dephosphorylation cycles coupled through regulatory interactions is driven by an independent oscillator producing repetitive pulses of cyclic AMP.

2. Model for a Cyclically Organized Network of Phosphorylation–dephosphorylation Cycles

The model considered is schematized in Fig. 1. It consists of a number N of covalent modification cycles in which a protein Y_i is transformed (phosphorylated) into the form X_i by an enzyme E_i (a kinase) of maximum rate V_{Mi} and Michaelis constant K_i, while the reverse transformation of X_i into Y_i is catalysed by an enzyme E'_i (a phosphatase) of maximum rate V'_{Mi} and Michaelis constant K'_i. The modification reactions involve cofactors (see Fig. 1, right panel) whose concentrations will be considered as remaining constant. The forms X_i and Y_i may represent active and inactive forms of a protein, respectively. We shall

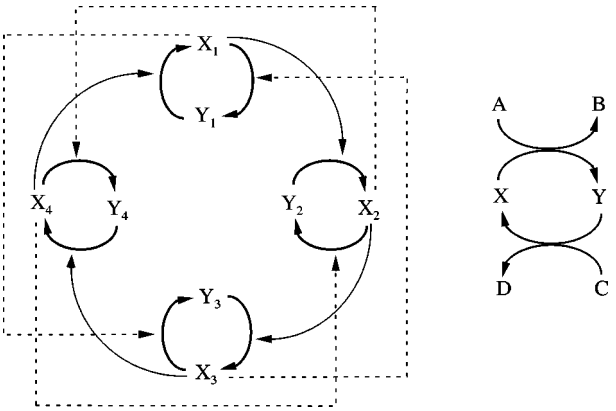

FIG. 1. Scheme of the model for a network of coupled phosphorylation–dephosphorylation cycles (left panel) displaying the dynamics of dominoes and clocks. The network represented contains four cycles in which protein Y_i is phosphorylated into the form X_i. In each cycle cofactors are involved (right panel): phosphorylation by a kinase is accompanied by hydrolysis of ATP (A) into ADP (B), while dephosphorylation by a phosphatase is accompanied by consumption of H_2O (C) and production of inorganic phosphate, P_i (D). The model applies to other modes of covalent modification, and also to the case where one or more species X_i represent dephosphorylated forms of these proteins. The various cycles of the network are coupled through forward (——) and backward (– – –) regulatory interactions. Thus, we assume that X_i activates both the enzyme converting Y_{i+1} into X_{i+1}, and the enzyme converting X_{i-2} into Y_{i-2}. These cyclically organized regulatory interactions give rise to oscillatory behavior. Because of its cyclical structure, the model could be referred to as the *circulator*.

illustrate the results mostly for a network of four such covalent modification cycles ($N = 4$), but have studied the effect of increasing the number of cycles in the network.

Each form X_i activates the next step in the network, i.e. the reaction transforming Y_{i+1} into X_{i+1}. The cyclical nature of the network arises from the hypothesis that in a network containing N interconversion steps, the product of the last step, X_N, activates the conversion of Y_1 into X_1. With only such positive regulatory interactions, no oscillations are possible and only bistability is observed: either the system is turned on, or it remains turned off (see Section 5). To allow for the possibility of periodic behavior we have incorporated the hypothesis that each species X_i can exert a negative feedback on a preceding cycle in the network. Thus we assume, for example, that species X_{i+2} activates the enzyme that transforms X_i back into the form Y_i. For the two types of regulation, we shall assume that the enzymes possess a residual activity in the absence of their activator (case of non-essential activation). The network model thus defined could be referred to as the *circulator*, to underline its cyclical organization.

We shall denote by X_i the fraction of protein X_i. Assuming that the complexes of X_i and Y_i with the modifying enzymes remain negligible, X_i is thus defined by $X_i = [X_i]/([X_i] + [Y_i])$, with $Y_i = 1 - X_i$. Because of the symmetrical nature of the scheme considered, the time evolution of the fractions X_i is given in a compact form by the following vectorial equation:

$$\frac{dX_i}{dt} = V_i \frac{(1-X_i)}{K_i + (1-X_i)} - V_i' \frac{X_i}{K_i' + X_i} \quad (i = 1, \ldots, N) \tag{1}$$

with

$$V_i = V_{Mi}\left(1 + \alpha_i \frac{X_{i-1}}{K_{ai} + X_{i-1}}\right),$$

$$V_i' = V_{Mi}'\left(1 + \beta_i \frac{X_{i+2}}{K_{bi} + X_{i+2}}\right). \tag{2}$$

Owing to the cyclical nature of the network, in eqns (2), $X_{i-1} \equiv X_N$ for $i = 1$, $X_{i+2} \equiv X_1$ for $i = N - 1$, and $X_{i+2} \equiv X_2$ for $i = N$. Indeed, X_{i-1} and X_{i+2} refer, respectively, to the intermediates located one step before and two steps after X_i in the cyclical network.

In the above equations, α_i and β_i represent coefficients measuring the strength of regulatory coupling in the network: the maximum activity of the modifying enzymes is multiplied by a factor $(1 + \alpha_i)$ or $(1 + \beta_i)$ in the presence of such a regulation when the effector is much larger than the activation constant K_{ai} or K_{bi}. Parameters V_{Mi}, K_i, V_{Mi}', K_i' are normalized by division through the total amount of the corresponding substrate protein.

3. Unifying the Dynamics of Dominoes and Clocks

A key feature of the model considered is that thresholds may arise in each of the covalent modification cycles interconverting Y_i into X_i. The dependence of the steady-state fraction of X_i as a function of the ratio V_i/V_i' of maximum

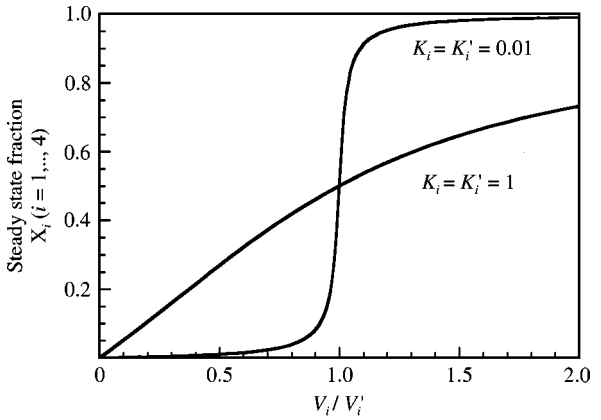

FIG. 2. Threshold in a single phosphorylation–dephosphorylation cycle. Shown is the steady-state fraction of phosphorylated protein X_i as a function of the ratio of maximum rates of phosphorylation (V_i) and dephosphorylation (V_i'). When the reduced Michaelis constants of the kinase (K_i) and phosphatase (K_i') are much smaller than unity (e.g. $K_i = K_i' = 0.01$), the curve presents a sharp threshold due to the phenomenon of zero-order ultrasensitivity (Goldbeter & Koshland, 1981). Such a threshold is not observed at higher values of the reduced Michaelis constants (e.g. $K_i = K_i' = 1$).

rates becomes highly sigmoidal when the reduced Michaelis constants K_i and K_i' are much smaller than unity. Thus, the sharp threshold seen for $K_i = K_i' = 0.01$ disappears when $K_i = K_i' = 1$ (see Fig. 2). We shall make use of this property, called zero-order ultrasensitivity (Goldbeter & Koshland, 1981, 1982), to generate thresholds in each step of the network of Fig. 1. In the following, we shall use the values $K_i = K_i' = 0.01$ unless indicated otherwise.

In plotting the curves yielding the steady-state fraction of X_i as a function of the ratio V_i/V_i' we did not consider explicitly how this ratio varies with the regulatory interactions described by eqns (2). In the present model we first consider the case (see Fig. 1 and Section 2) where each species X_i activates the next transformation of Y_{i+1} into X_{i+1} as well as the reverse transformation, two cycles earlier in the network, of X_{i-2} into Y_{i-2}. The latter assumption introduces a delay necessary for the occurrence of sustained oscillations; when X_i activates the transformation of X_{i-1} into Y_{i-1} in the preceding cycle, only damped oscillations occur. In the following, we will focus on the time evolution of the various species X_i. Oscillations in X_i are always accompanied by periodic variation in the corresponding Y_i species, according to the conservation relation $Y_i = 1 - X_i$.

For appropriate parameter values (see below) the network of phosphorylation–dephosphorylation cycles shown in Fig. 1 behaves both as a limit-cycle oscillator and as a repetitive sequence of domino-like transitions. Starting from the immediate vicinity of the unstable steady state, we see that the four variables of the system are successively turned on and off in an abrupt manner [Fig. 3(a)]. In the phase plane (X_1, X_2) these sustained oscillations correspond to a limit cycle; the nearly square shape of this trajectory [Fig. 3(b)] is due to the fact that the rise and decline of one variable occur at nearly constant values of the preceding or following variable. In the absence of very sharp thresholds, e.g. at the higher values $K_i = K_i' = 0.03$ which are close to the upper limit of the oscillatory domain [see Fig. 6(a)], oscillations still occur but are much smoother [Fig. 3(c)] and correspond to a more rounded limit cycle [Fig. 3(d)].

The conditions in which sustained oscillations occur in the model can be determined by means of bifurcation diagrams established with respect to one or two parameters. Shown in Fig. 4 is a bifurcation diagram representing the steady state (stable or unstable) and the envelope of oscillations as a function of the ratio of maximum rates $r = V_M/V_M'$ in the fully symmetrical case where all phosphorylation–dephosphorylation cycles are characterized by the same set of parameter values. The bifurcation diagram indicates that sustained oscillations occur in a domain corresponding to the range of steep increase in the steady-state fractions X_i ($i = 1, \ldots, 4$); the domain of instability of the steady state (dashed line) is bounded by two critical values of parameter r which correspond to subcritical Hopf bifurcations. Near the bifurcation points a domain of hard excitation indeed exists in which a stable steady state coexists with a stable limit cycle.

The dynamic consequences of hard excitation are illustrated in Fig. 5. Starting at the stable steady state (where $X_1 = X_2 = X_3 = X_4$ in the symmetrical case considered) we increase at time $t = 20$ parameter V_{M1} from 0.85 up to 2 during 10 units of time before returning V_{M1} to its initial

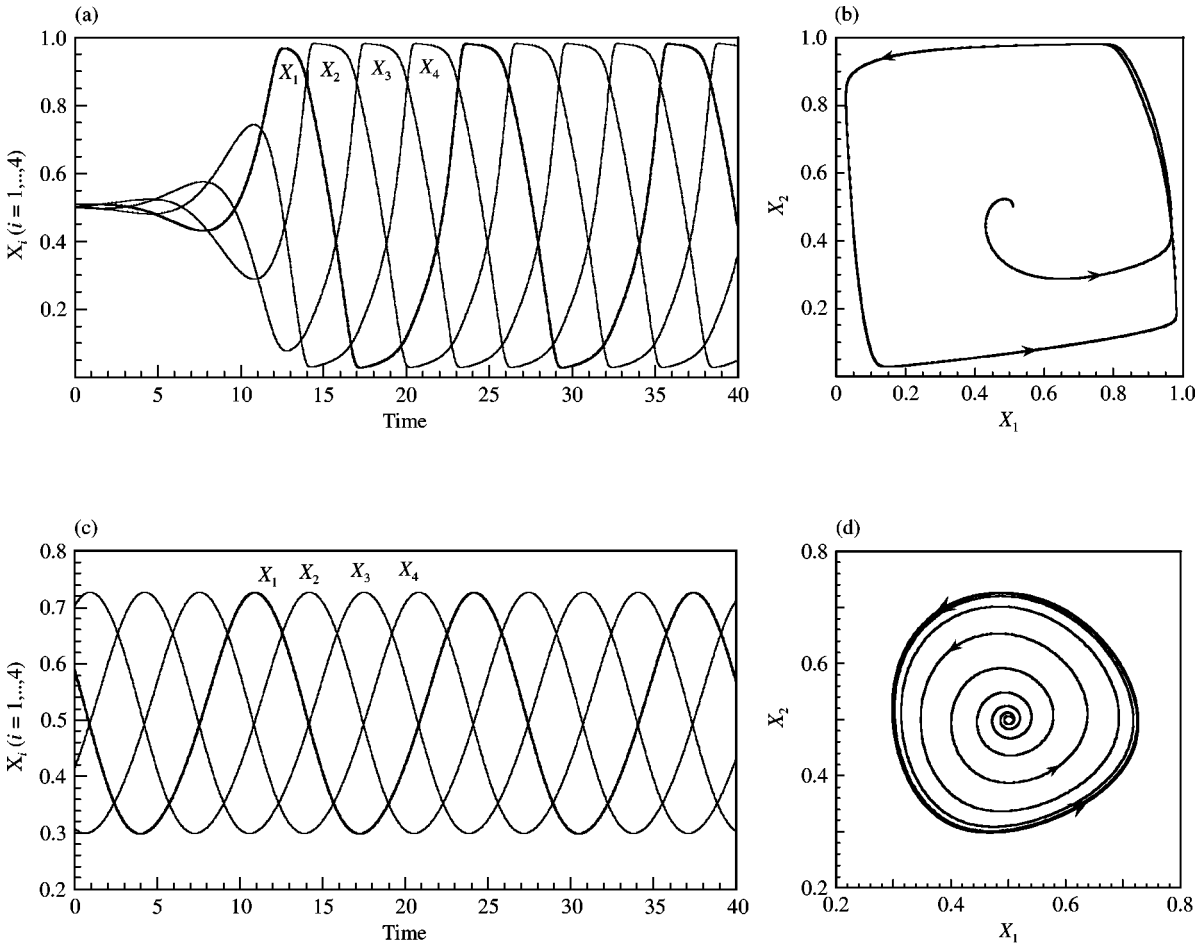

FIG. 3. Unifying the dynamics of dominoes and clocks. Sustained oscillations obtained for $K = K' = 0.01$ and 0.03 are shown in (a) and (c), respectively. The corresponding limit cycles in the (X_1, X_2) plane are shown in (b) and (d). The oscillations in (a) resemble a recurrent sequence of rising and falling dominoes, while the oscillations in (c) are much smoother. Consequently, the limit cycle in (d) corresponding to the latter oscillations is much rounder than the square limit cycle in (b) associated with the oscillations in (a). The results are obtained by numerical integration of eqns (1) for a network containg four phosphorylation–dephosphorylation cycles, as shown in Fig. 1. Other parameter values (corresponding to the symmetrical case) are $\alpha_i = \beta_i = 1$, $K_{ai} = K_{bi} = 0.5$, $V_{Mi} = V'_{Mi} = 1$ (in the present and following figures, these normalized maximum rates are expressed in arbitrary time units^{-1}), for $i = 1, \ldots, 4$. Initial conditions: $X_1 = 0.51$, $X_2 = X_3 = X_4 = 0.5$; transients have been suppressed in panel (c).

value [Fig. 5(a)]. As a result of this transient increase in the maximum phosphorylation rate in the first cycle of the sequence the system switches to a regime of sustained oscillations and continues to oscillate despite the return of parameter V_{M1} to its initial value. The reverse transition is illustrated in Fig. 5(b) where the system starts in the oscillatory state. At time $t = 20$ parameter V_{M1} is decreased transiently from 0.85 down to 0.5, before being returned to its initial value at time $t = 30$. In spite of the transient nature of the parameter change, the system has permanently switched toward the stable steady state. The transitions illustrated in panels (a) and (b) of Fig. 5 are direct consequences of the coexistence between a stable steady state and a stable limit cycle in conditions of hard excitation.

Stability diagrams established for different pairs of parameters are shown in Fig. 6. In each diagram a domain of sustained oscillations is indicated, besides domains in which the network evolves toward a stable steady state. A domain of hard excitation sometimes exists near the boundary of the oscillatory domain, as shown in (b) and (c). Panels (a) and (c) show that for sustained oscillations to occur, the values of the reduced

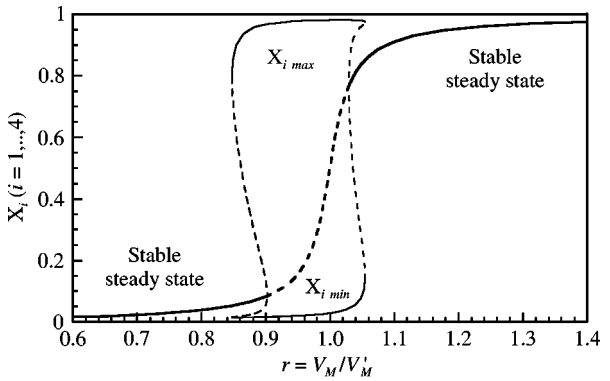

FIG. 4. Bifurcation diagram showing the domain of sustained oscillations as a function of the ratio of kinase to phosphatase maximum rates, in a network containing four phosphorylation–dephosphorylation cycles with both forward and backward coupling. The curves show the stable (———) or unstable (-------) steady state, as well as the envelope of the oscillations, as a function of the ratio $r = V_M/V'_M$ which is taken as identical in the four cycles of the network. At both extremities of the oscillatory domain unstable limit cycle oscillations (dashed line) separate the stable oscillations from the stable steady state. Parameter values are as in Fig. 3(a). The ratio $r = V_M/V'_M$ is varied by changing V'_M at the fixed value $V_M = 1$.

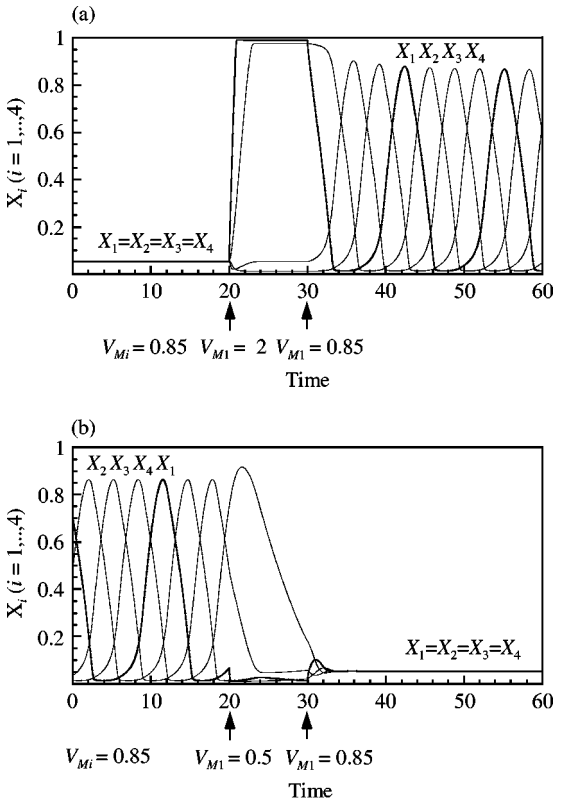

FIG. 5. Dynamic consequences of the coexistence between a stable steady state and stable oscillations (*hard excitation*). (a) Transition from the stable steady state to the stable oscillatory regime following a transient perturbation in parameter V_{M1} which is increased from 0.85 to 2 from $t = 20$ to 30 and is thereafter returned to its initial value. (b) Transition from the stable oscillatory regime to the stable steady state following a transient perturbation in parameter V_{M1} which is decreased from 0.85 to 0.5 from $t = 20$ to 30 before being returned to its initial value. As can be seen in Fig. 4, a stable steady state and a stable limit cycle coexist when $V_{M1} = 0.85$. Other parameter values are as in Fig. 3(a), with $V_{Mi} = 0.85$ $(i = 2, \ldots, 4)$. Initial conditions are (a) $X_i = 0.053$ $(i = 1, \ldots, 4)$, (b) $X_1 = 0.023$, $X_2 = 0.044$, $X_3 = 0.822$, $X_4 = 0.279$.

Michaelis constants $K_i = K'_i = K$ must be sufficiently small, i.e. the transition curves for each fraction of phosphorylated protein must be sufficiently steep (see Fig. 2). The diagram of panel (c) extends the results of Fig. 4 by showing the existence of a range of values of $r = V_M/V'_M$ in which sustained oscillations occur. Panel (b) indicates that in the symmetrical case, the value of β must exceed the value of α for oscillations to occur.

Sustained oscillations in the phosphorylation–dephosphorylation network model can also be observed in asymmetrical conditions, as shown in Fig. 7(a) where each cycle of phosphorylation–dephosphorylation is characterized by different values of parameters V_M and α. As a result, the amplitude and waveform differs for each of the variables of the system. It is possible to uncouple one of the variables from the rest of the system and to nevertheless obtain oscillations in all the other variables of the network. Thus, Fig. 7(b) shows the behavior of the network model of Fig. 1 when $\alpha_1 = \beta_1 = 0$, i.e. when X_1 is uncoupled from the rest of the network; see eqns (1) and (2). The reason why we still observe oscillations is due to the fact that the link between X_4 and X_2 is not interrupted, because of the assumption that X_{i+1} activates the transformation of Y_{i-1} into X_{i-1}: the backward regulation jumps over one step in the network of phosphorylation–dephosphorylation cycles.

The model can display a rich repertoire of dynamic behavior which will only briefly be mentioned here. Besides the type of oscillations shown in Fig. 3, more complex patterns of oscillatory behavior can indeed occur in the presence of forward and backward coupling when the network contains more than six phosphorylation–dephosphorylation cycles. Thus, for $N = 7$, depending on the value of $\beta > \alpha$, oscillations can be found in which peaks in $X_1, X_5, X_2, X_6, X_3, X_7$,

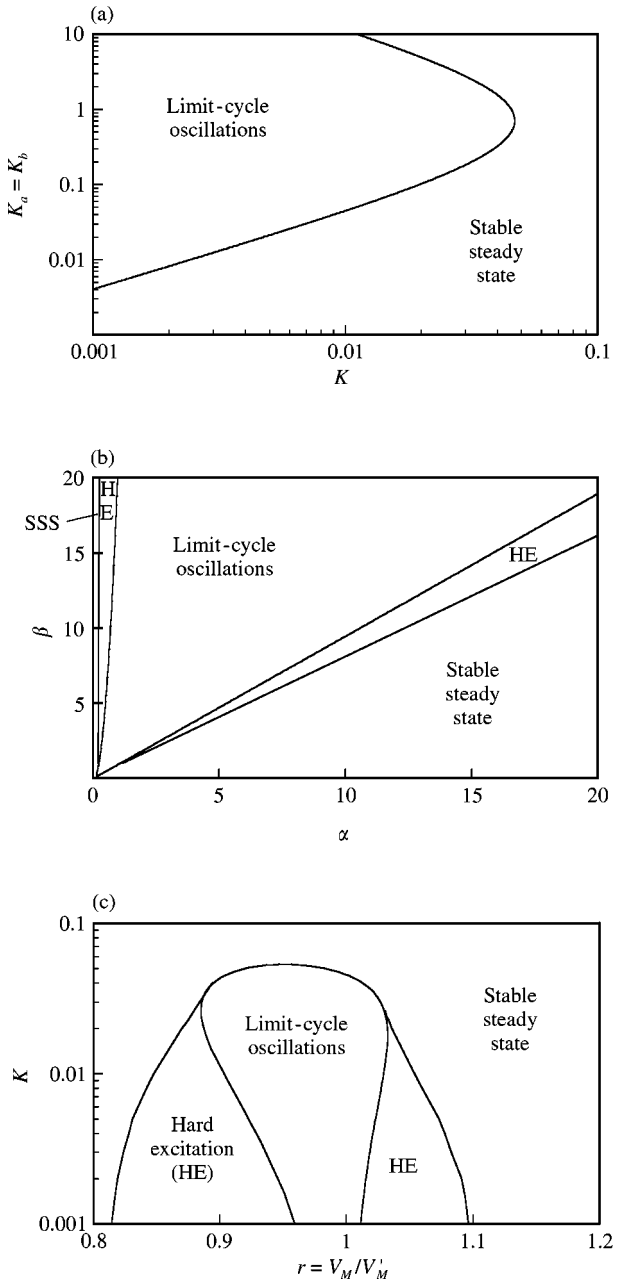

FIG. 6. Two-parameter diagrams showing the domain of sustained oscillations in a network containing four phosphorylation–dephosphorylation cycles with both forward and backward coupling. The diagrams are obtained in the symmetrical case where $K_i = K$, $K_{ai} = K_a$, $K_{bi} = K_b$, $\alpha_i = \alpha$, $\beta_i = \beta$, $V_{Mi} = V_M$, $V'_{Mi} = V'_M$ $(i = 1, \ldots, 4)$, for the parameter values of Fig. 3(a). Panels (a)–(c) show the domains of limit-cycle oscillations and of stable steady states (SSS) in the parameter planes $K_a = K_b$ vs. K, α vs. β, K vs. $r = V_M/V'_M$, respectively. In panels (b) and (c) a domain of hard excitation (HE) in which a stable steady state coexists with a stable limit cycle sometimes exists near the boundaries of the oscillatory domain (see Fig. 4). Parameter r in (c) is varied through V'_M as in Fig. 4.

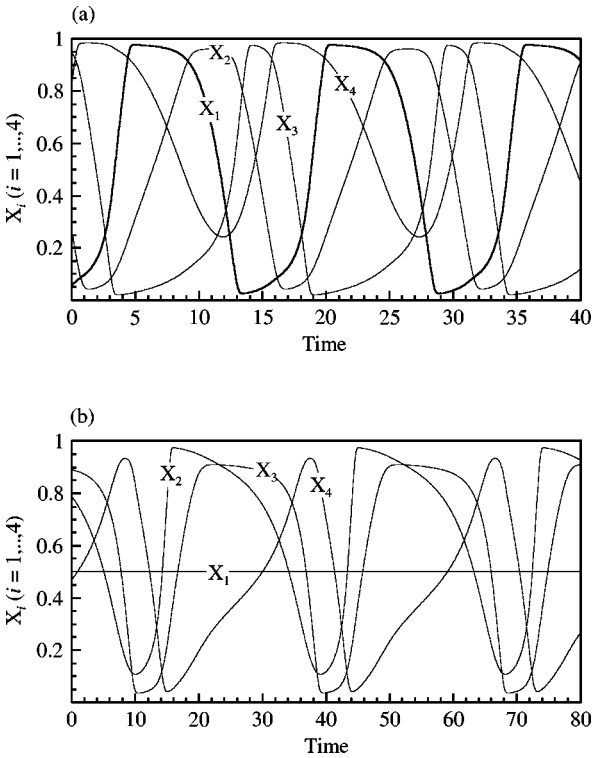

FIG. 7. Sustained oscillations in asymmetrical conditions, in the presence of both forward and backward coupling. Parameter values are: (a) $V_{M1} = 0.6$, $V_{M2} = 1.2$, $V_{M3} = 0.8$, $V_{M4} = 1.4$, $\alpha_1 = 2.3$, $\alpha_2 = 0.7$, $\alpha_3 = 1.5$, $\alpha_4 = 0.4$. (b) $V_{Mi} = 1$ $(i = 1, \ldots, 4)$, $\alpha_1 = \beta_1 = 0$, $\alpha_i = \beta_i = 1$ $(i = 2, \ldots, 4)$. Other parameter values are as in Fig. 3(a). In (b), X_1 does not oscillate because it is actually uncoupled from the rest of the network since $\alpha_1$and β_1 are both nil. However, the remaining variables remain coupled through regulatory interactions. The backward regulations exerted by X_2 on X_4 and by X_4 on X_2, and the forward regulation exerted by X_2 on X_3 indeed operate and allow oscillations in X_2, X_3 and X_4.

X_4, X_1 successively occur. Such alternating oscillations coexist, for some values of β/α, with simple sequential oscillations of the type shown in Fig. 3. For $N = 8$ and $\beta > \alpha$, oscillations can be grouped into two sets of variables, with successive peaks in $X_1 = X_5$, $X_2 = X_6, \ldots, X_4 = X_8$. Again, these oscillations can sometimes coexist with the simple alternating oscillations of the type shown in Fig. 3; only the latter type of oscillations are found when $\alpha > \beta$. These results extend to larger, odd or even values of N.

4. Holding a Domino and Arresting the Clock

The question arises as to whether the clock can readily be stopped by preventing one of the

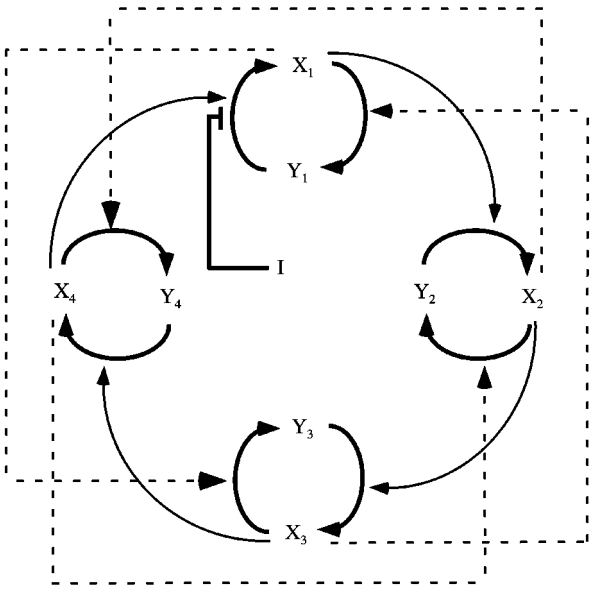

FIG. 8. Action of an inhibitor in the network of coupled phosphorylation–dephosphorylation cycles shown in Fig. 1. Here I is a kinase inhibitor that reduces the maximum rate of conversion of Y_1 into X_1.

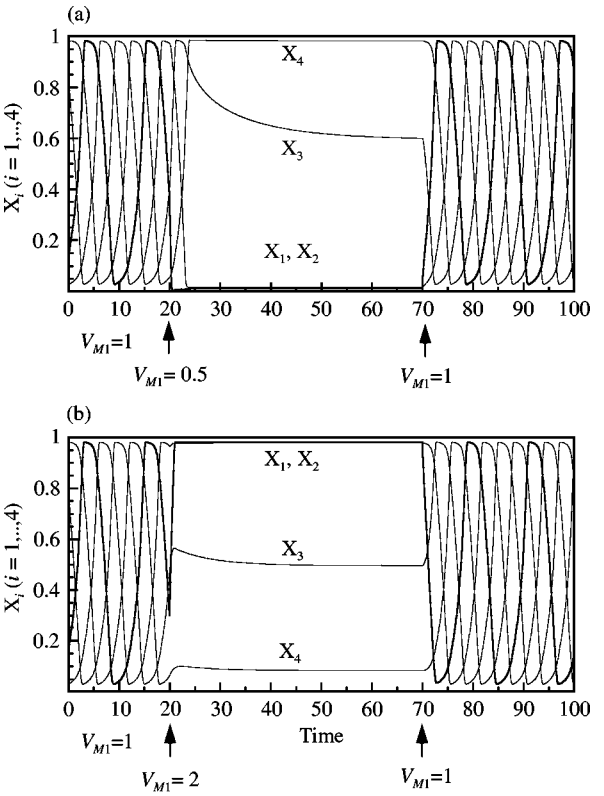

FIG. 9. (a) Immediate arrest of the oscillations when the inhibitor I in the system shown in Fig. 8 reduces the maximum rate V_{M1} by a factor of 2 in $t = 20$ (first arrow); the oscillations resume as soon as the inhibition is lifted and V_{M1} recovers its initial value in $t = 70$ (second arrow). (b) Similar effects can be observed when the maximum rate V_{M1} is increased by a factor of 2 (first arrow) and later brought back to its initial value (second arrow), as a result of the addition and subsequent removal of some kinase activator. Parameter values are as in Fig. 3(a).

domino-like transitions in the network of phosphorylation–dephosphorylation cycles. To assess this possibility, we consider the presence of an inhibitor which reduces by 50% the maximum rate V_{M1} of conversion of Y_1 into X_1 (Fig. 8) and thereby holds the system to the left of the threshold characterizing the transition of Y_1 into X_1 (Fig. 2). The result of such an inhibition is the immediate arrest of the oscillations and the concomitant evolution toward a steady state characterized by low values of X_1 and X_2, a high value of X_4 and an intermediate value of X_3 [Fig. 9(a), left arrow]. As soon as the inhibitor is removed and parameter V_{M1} recovers its initial value, the oscillations resume [Fig. 9(a), right arrow]. The same effects can also be obtained if, instead of dividing by a factor of 2 the value of V_{M1}, the value of V'_{M1} is multiplied by the same factor.

Because sustained oscillations occur in a domain bounded by two critical values of the ratio V_{M1}/V'_{M1}, the arrest of the clock can also be achieved by increasing rather than decreasing parameter V_{M1}. Then, as shown in Fig. 9(b) (left arrow), oscillations immediately stop and the system evolves toward a steady state characterized by high values of X_1 and X_2, a low value of X_4 and an intermediate value of X_3. The oscillations resume as soon as the parameter recovers its initial value [Fig. 9(b), right arrow]. Here again similar effects are obtained if the increase in V_{M1} is replaced by a decrease in V'_{M1}.

To better understand the way the clock is stopped by an instantaneous change in one of the control parameters, it is useful to consider the dynamics in the phase space resulting, for example, from a two-fold decrease in parameter V_{M1}. Shown in Fig. 10 are the trajectories (dashed lines) resulting from such a change, for various initial conditions corresponding to five different points on the limit cycle (open circles marked 1–5). The change considered in Fig. 9(a) (left arrow) corresponds to the case where the reduction in V_{M1} occurs in point 1. In all cases the

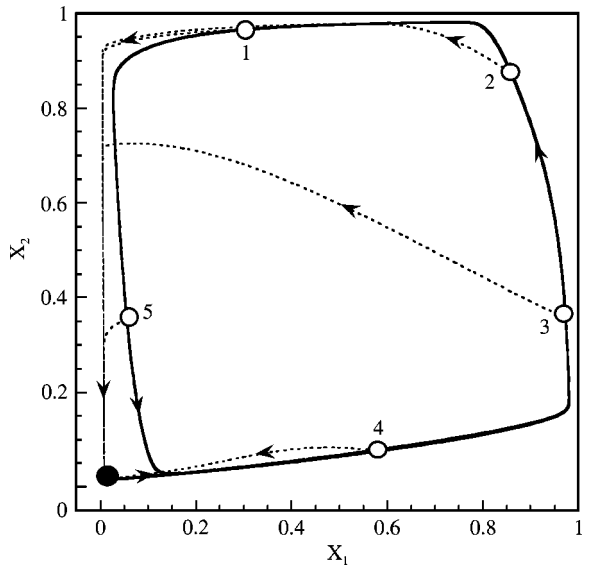

FIG. 10. Suppression of sustained oscillations in the phase plane. Starting from five points (denoted 1–5) of the limit cycle shown as a projection in the (X_1, X_2) plane, the network of phosphorylation–dephosphorylation cycles represented in Fig. 8 evolves right away toward the steady state (black dot) when the maximum rate V_{M1} is reduced by a factor of 2. The trajectory starting from point 1 corresponds to the arrest of the oscillations shown in Fig. 9(a). When the initial value of V_{M1} is restored, the system immediately returns (solid arrowed line) to the limit cycle.

system responds to the decrease in V_{M1} by evolving immediately toward the steady state (black dot). When the parameter recovers its initial value, the system directly resumes its periodic motion along the limit cycle (arrowed solid line starting from the steady state). Similar results are obtained when increasing V'_{M1}, and more generally, when controlling any of the other steps of the network.

Figures 9 and 10 demonstrate that the limit-cycle behavior can readily be brought to a stop when the system is prevented from passing through one of the thresholds associated with each of the phosphorylation–dephosphorylation cycles of the network. Thus, holding any of the dominoes brings the system to a halt; in dynamical terms, this corresponds to the evolution from the limit cycle to the stable steady state that is reached for the new value of parameter V_{M1}. Preventing the progression through the successive transitions in the network therefore amounts to holding the dominoes in place and to arresting the clock by putting a spoke in the limit-cycle wheel. The temporary arrest of oscillations lasts as long as the inhibitor is present, and limit-cycle behavior resumes as soon as the inhibitor is removed. The arrest of the clock occurs because the sequence of domino-like transitions itself constitutes the clock.

5. Dynamics of the Network with only Backward or Forward Coupling

The network studied so far contains two types of regulatory coupling (see Fig. 1): each species X_i (a) activates the next step in the network by enhancing the rate of conversion of Y_{i+1} into X_{i+1} (forward coupling) and (b) controls a previous step by enhancing the conversion of X_{i-2} into Y_{i-2} (backward coupling). The question arises as to what is the dynamic behavior of a network model in which only the forward or the backward type of coupling is present. These two situations can readily be implemented by setting equal to zero the parameters β_i or α_i ($i = 1, \ldots, N$), respectively.

Model networks containing four phosphorylation–dephosphorylation cycles and subjected only to forward or backward coupling are represented in the left and right panels of Fig. 11. The dynamics of the two types of network differs markedly. In the case of only forward coupling, oscillations are never obtained; instead, the system displays the property of bistability (Fig. 12, left column). In the symmetrical case where all cycles possess the same parameter values, a range of $r = V_M/V'_M$ exists in which two stable steady states, separated by an unstable steady state, coexist. Then, depending on the initial conditions, the network evolves toward a state in which all X_i ($i = 1, \ldots, 4$) are either high [Fig. 12(b)] or low [Fig. 12(c)]. The X_i vs. r curve possesses a characteristic S-shape [Fig. 12(a)] which is associated with hysteresis as parameter r is varied back and forth over the bistability range.

The situation in the presence of only backward coupling is different and depends on the number of cycles in the network. When the network consists of four phosphorylation–dephosphorylation cycles, multistability is observed but in a different way than in Fig. 12(a)–(c): the bifurcation diagram showing the steady-state value of X_i as

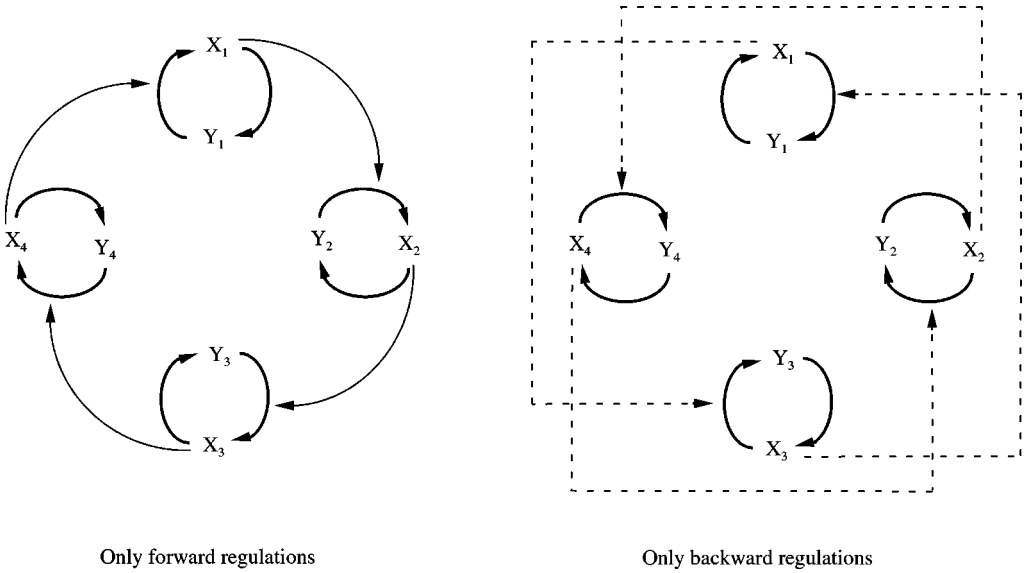

FIG. 11. Scheme of a network containing four phosphorylation–dephosphorylation cycles in the presence of only forward or backward coupling.

a function of $r = V_M/V'_M$ is of the pitchfork type [Fig. 12(d)]. Here, four different steady-state situations are possible, because of the actual uncoupling of the subsets containing, respectively, the (X_1, Y_1), (X_3, Y_3) and the (X_2, Y_2), (X_4, Y_4) cycles which are linked two by two through regulatory interactions. Thus, the system evolves to a steady state in which X_1, X_2 are high and X_3, X_4 are low [Fig. 12(e)], to another steady state in which X_1, X_4 are high and X_2, X_3 are low [Fig. 12(f)], or to steady states corresponding to the reverse configurations (not shown).

In the presence of only backward coupling, another type of behavior can, however, be observed when the network contains an odd number of cycles. The situation of a five-cycle network controlled by only backward regulations is represented in Fig. 13. In such a system, sustained oscillations occur in an appropriate range of parameter values (Fig. 14) and the behavior is analogous to that seen in the system containing both backward and forward coupling [see Fig. 3(a)].

The results on the effect of negative, backward and/or positive, forward coupling have been generalized to networks containing more than 5 cycles of phosphorylation–dephosphorylation. The results are summarized in Table 1 in section 7 below. When both forward and backward coupling are present, sustained oscillations can occur regardless of the value of the number of cycles N, for $N > 3$. In the presence of only positive, forward coupling, bistability with hysteresis can occur regardless of the value of N, with all variables having relatively high or low values [see Fig. 12(a)–(c)].

When only negative, backward coupling is considered, sustained oscillations can occur when N or $N/2$ are odd numbers (this stems from the assumption that backward coupling is exerted by variable X_i on step $(i - 2)$ in the network). If $N/2$ is an even number, bistability of the pitchfork type [with half of the variables at a high value and the remaining half at a relatively low value; see Fig. 12(d)–(f)] can be observed. Because of the existence of two independent subsets containing $N/2$ coupled cycles, four different stable steady states can be obtained in these conditions, when taking into account the different possible combinations [see Fig. 12(e) and (f) for the case $N = 4$]. When N is even and $N/2$ is odd, oscillations occur in two uncoupled subsets of $N/2$ different X species. Thus, for $N = 10$, oscillations occur in (X_1, X_3, X_5, X_7, X_9) and, independently, in (X_2, X_4, X_6, X_8, X_{10}) with a phase relationship that is only dictated by initial conditions.

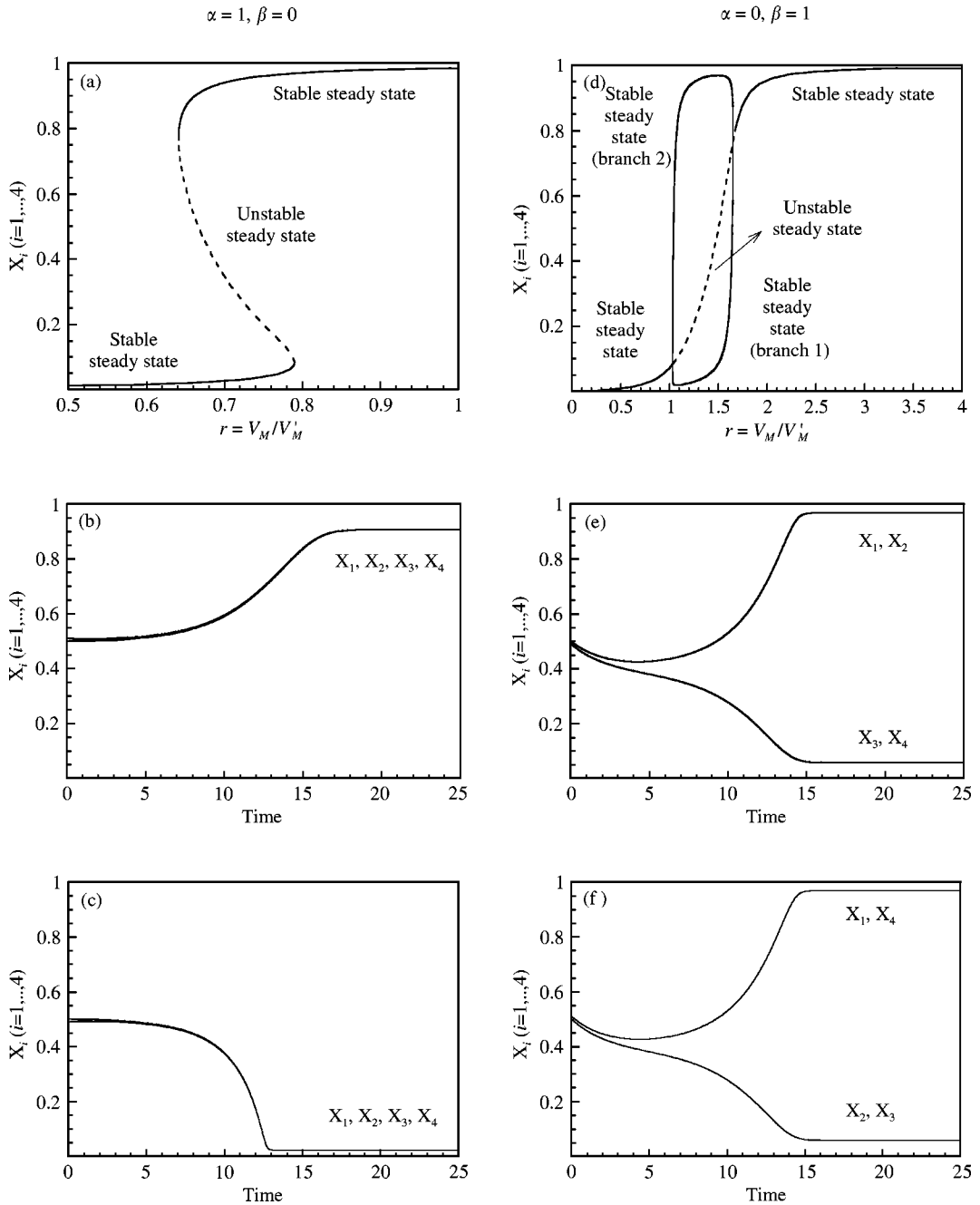

FIG. 12. Bistability in the presence of only forward (left column) or backward (right column) coupling. The curves are obtained in the symmetrical case for the models schematized in Fig. 11. In the presence of only forward coupling, the coexistence of two stable steady states, in which all X_i are equal and either high (b) or low (c), corresponds to an S-shaped curve (a) as a function of $r = V_M/V'_M$; the two stable states are separated by an unstable steady state (– – –). In the presence of only backward coupling, bistability is of the pitchfork type (d) as the coexisting stable steady states, again separated by an unstable steady state (– – –), correspond to large values of some intermediates X_i, and low values of the others. In the symmetrical case considered the system shown in the right panel of Fig. 11 consists of two independent parts containing the (X_1, Y_1), (X_3, Y_3) and (X_2, Y_2), (X_4, Y_4) cycles, respectively. Four possible steady-state situations can be encountered, in which X_1, X_2 are high and X_3, X_4 are low (e), or X_1, X_4 are high and X_2, X_3 are low (f); the additional two cases correspond to the reverse situations (not shown). The values of α and β are indicated at the top of figure; $V_M = 1$; $V'_M = 1.5$ in (b) and (c) and $V'_M = 0.7$ in (e) and (f). Other parameter values are as in Fig. 3(a). Initial conditions are $X_3 = X_4 = 0.5$ with (b) $X_1 = 0.51$, $X_2 = 0.5$, (c) $X_1 = 0.49$, $X_2 = 0.5$, (e) $X_1 = X_2 = 0.49$, (f) $X_1 = X_2 = 0.51$.

6. Dominoes Linked to an Independent Clock

So far we focused on a model that displays the dynamics of dominoes and clocks. To understand in further detail the link between the two types of behavior, it is useful to consider a model where a sequence of domino-like transitions is capable of oscillating only when coupled to an independent clock. The comparison between the two models will help to contrast the two situations and to pinpoint ways to distinguish between them.

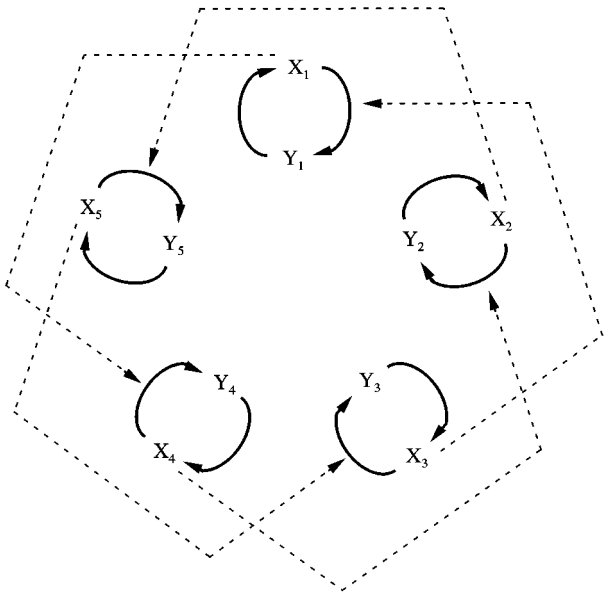

FIG. 13. Scheme of a network of five phosphorylation–dephosphorylation cycles coupled only through backward regulatory interactions.

For definiteness we consider a model, schematized in Fig. 15, in which a linear sequence of three coupled phosphorylation–dephosphorylation cycles is linked to an independent biochemical oscillator producing repetitive pulses of cyclic AMP (cAMP). Each pulse of cAMP triggers the activation of the kinase acting in the first cycle of the cascade, in which a protein Y_1 is phosphorylated into the form X_1 by a kinase E_1 of maximum rate V_{M1} and Michaelis constant K_1. We assume that X_1 is an enzyme that catalyses the synthesis of an intermediate Z_1 which itself activates a kinase acting in the transformation of Y_2 into X_2 in the second cycle of the network. A similar link with a third phosphorylation–dephosphorylation cycle is considered through an intermediate Z_2. Similar results would be obtained if the kinases acting in the second and third cycles were directly activated by X_1 and X_2, respectively, as in the model of Fig. 1. However, the transient changes in X_1, X_2, and X_3 triggered by cAMP oscillations are better separated when the activation of the kinases occurs via the intermediates Z_1 and Z_2.

The linear sequence of phosphorylation–dephosphorylation cycles considered in this model cannot by itself generate oscillations. It can, however, display oscillations when it becomes coupled to the cAMP oscillator which behaves as an independent clock. For illustrative purposes, we will use for the cAMP oscillator a theoretical

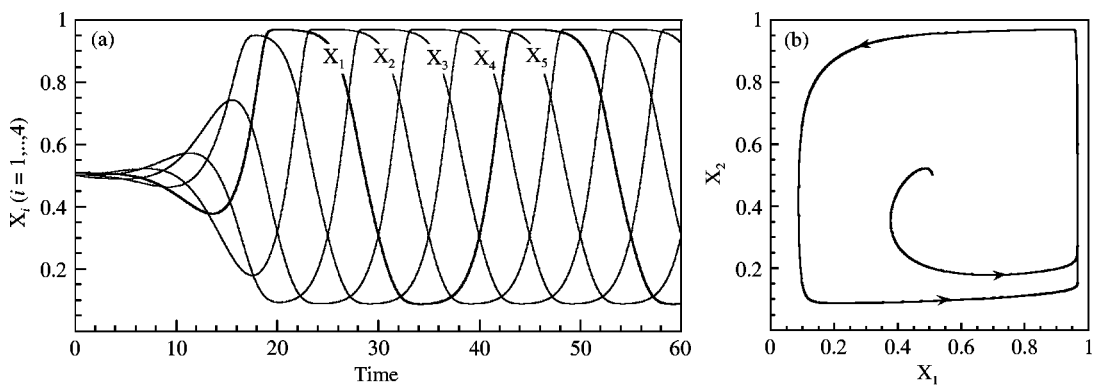

FIG. 14. Sustained oscillations in the presence of only backward coupling in the model schematized in Fig. 1. (a) Time evolution, and (b) limit-cycle projection in the (X_1, X_2) plane. The curves are obtained by numerical integration of eqns (1), with $N = 5$ and $\alpha_i = 0$, $\beta_i = 1$, $V_{Mi} = 1.5$; $V'_{Mi} = 1$ $(i = 1, \ldots, 5)$. Other parameter values are as in Fig. 3(a). Initial conditions: $X_1 = 0.51$, $X_2 = \cdots = X_5 = 0.5$.

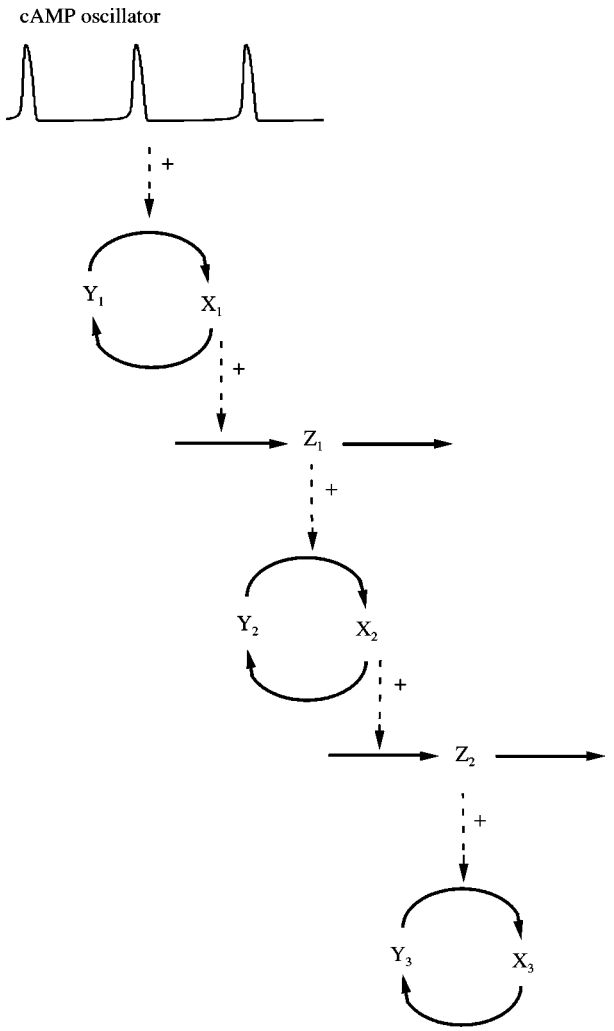

FIG. 15. Model of a linear sequence of phosphorylation–dephosphorylation cycles, passively coupled to an independent oscillator generating repetitive pulses of cyclic AMP. We assume that the oscillator drives phosphorylation of Y_1 into X_1 in the first cycle through activation of a cAMP-dependent protein kinase (see text for details).

model previously proposed for pulsatile cAMP signaling in *Dictyostelium discoideum* amoebae (Goldbeter & Segel, 1977; Goldbeter, 1996). Other models for cAMP oscillations could be used (e.g. the one proposed by Martiel & Goldbeter, 1987) without changing the nature of the results; the present analysis, indeed, remains largely independent of details of the oscillator kinetics. The cAMP oscillator could likewise be replaced by a calcium oscillator which could also control a phosphorylation–dephosphorylation cascade through modulation of a Ca^{2+}-activated kinase (Goldbeter *et al.*, 1990).

The model for cAMP oscillations in *D. discoideum* is governed by the three kinetic equations (3) which describe the time evolution of the concentrations of intracellular ATP, intracellular cAMP, and extracellular cAMP; these three variables are denoted by a, b and c, respectively [see Goldbeter & Segel (1977), and Goldbeter (1996), for further details on these equations and on the significance of the parameters]:

$$\frac{da}{dt} = v - \sigma\phi,$$

$$\frac{db}{dt} = q\sigma\phi - k_t b,$$

$$\frac{dc}{dt} = \frac{k_t b}{h} - kc \qquad (3)$$

with

$$\phi = \frac{a(1+a)(1+c)^2}{L + (1+a)^2(1+c)^2}.$$

Coupling the linear chain of phosphorylation–dephosphorylation cycles with the independently running cAMP oscillator is achieved by assuming that the first kinase, of rate V_1, is activated by cAMP. The time evolution of variables X_i $(i = 1, \ldots, 3)$ and Z_i $(i = 1, 2)$, which denote the concentrations of the corresponding species in the model of Fig. 15, are given by

$$\frac{dX_i}{dt} = V_i \frac{(1 - X_i)}{K_i + (1 - X_i)} - V_i' \frac{X_i}{K_i' + X_i} \quad (i = 1, \ldots, 3),$$

$$\frac{dZ_i}{dt} = k_z X_i - v_z \frac{Z_i}{K_z + Z_i} \quad (i = 1, 2) \qquad (4)$$

with

$$V_1 = V_{M1}\left(\frac{b}{K_b + b}\right),$$

$$V_i = V_{Mi}\left(\frac{Z_{i-1}}{K_{ai} + Z_{i-1}}\right) \quad (i = 2, 3),$$

$$V_i' = V_{Mi}' \quad (i = 1, \ldots, 3).$$

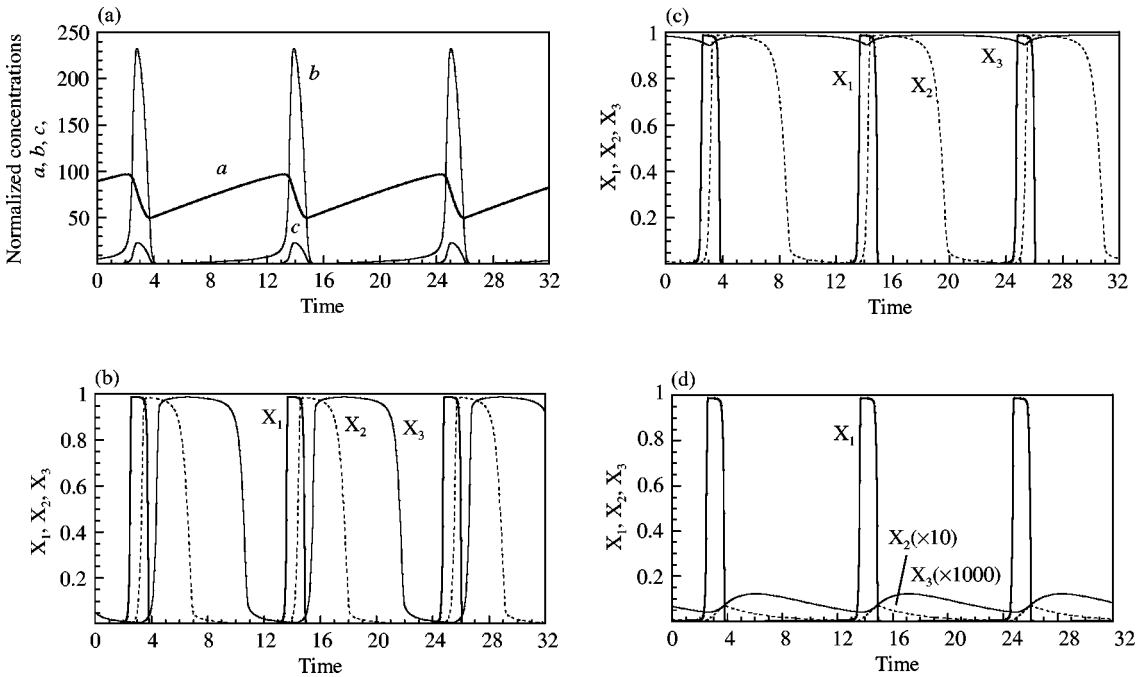

FIG. 16. Separating the dynamics of dominoes and clocks. In the model schematized in Fig. 15 and governed by eqns (3) and (4), repetitive domino-like transitions can occur in a system which does not behave as a clock, as a result of cyclic AMP oscillations (a) which run independently from the sequence of phosphorylation–dephosphorylation. The latter sequence is driven by these oscillations through the activation of a cAMP-dependent protein kinase in the first cycle of the network. (b) Oscillations of cAMP can elicit a repetitive sequence of domino-like transitions in all cycles of the network. Domino-like transitions can be prevented in the third cycle (c) or second cycle of the sequence (d), without affecting the transition in the first cycle. Data in panels (b–d) are obtained for the same oscillations of cAMP shown in (a). For the sake of clarity, the values of X_2 and X_3 in (d) have been multiplied by 10 and 10^3, respectively. Parameter values for the cAMP oscillations generated by eqns (3) are $\sigma = 1.2$, $v = 1.2$, $k = k_t = 0.4$, $L = 10^6$, $q = 100$, $h = 10$ (see Goldbeter & Segel, 1977; Goldbeter, 1996). Other parameter values are: (b) $V_{M1} = 0.5$, $V'_{M1} = 0.2$, $V_{M2} = 2$, $V'_{M2} = 0.2$, $V_{M3} = 3$, $V'_{M3} = 0.5$, $K_{a1} = K_{a2} = 0.5$, $k_b = 100$, $k_1 = k_2 = k_3 = 0.01$, $k_z = 0.0015$, $v_z = 0.002$, $K_z = 0.4$; (c) same as in (b) with $V_{M2} = 3$, $k_z = 0.001$, $v_z = 0.0014$; (d) same as in (b) with $V_{M2} = 0.5$ (time is expressed in arbitrary units).

The oscillations of intracellular cAMP (*b*) produced by this model are shown in Fig. 16(a). For our purpose, to retain generality, time is expressed in arbitray units (for the case of *Dictyostelium* cells it is expressed in minutes so that the period of cAMP oscillations is of the order of 10 min). How a sequence of domino-like transitions in the model schematized in Fig. 15 is passively coupled to independent cAMP oscillations is shown in Fig. 16(b). An increase in cAMP triggers an increase in X_1, which is followed, successively, by an increase in X_2 and in X_3. After each cAMP pulse, all variables of the phosphorylation–dephosphorylation network sequentially undergo a sharp rise followed by an abrupt fall. Here, however, in contrast to what is observed for the model analysed in the preceding sections, the chain of domino-like transitions can be interrupted without stopping the clock which continues to run independently. Two illustrations of this uncoupling are given in panels (c) and (d) of Fig. 16. Data in panels (b)–(d) were obtained in the presence of the same oscillations of cAMP [see panel (a)].

In Fig. 16(c), parameters are as in Fig. 16(b) except that the formation of X_2 from Y_2 is slightly favored. As a result, the plateau in X_2 lasts longer; this leads to a prolonged synthesis of effector Z_2, so that the ratio of phosphorylation vs. dephosphorylation rates in the third cycle of the network always exceeds the threshold value. As a consequence, X_3 always stays at a near-maximum value. This variable still oscillates, but only with a minute amplitude. If additional

phosphorylation–dephosphorylation cycles were coupled to the three cyles considered in Fig. 15, much as X_3 they would not display any domino-like transition.

Another way of uncoupling the clock from domino-like transitions is to prevent the passage through the phosphorylation–dephosphorylation threshold in one of the cycles of the network. Thus, in Fig. 16(d), the maximum rate of the kinase in the second cycle (V_{M2}) is divided by 4 as compared to the situation illustrated in panel (b). As a consequence, X_2 cannot pass its activation threshold and remains at a low value, while the next variable in the network, X_3, also fails to pass its threshold and remains at an even lower value. As indicated in Fig. 16(d), variables X_2 and X_3 have lost the property of undergoing domino-like transitions, but the oscillations in variable X_1 persist, being driven by the oscillations of cAMP which continue regardless of whether any passively coupled oscillations occur in the network of phosphorylation–dephosphorylation cycles.

A comparison of panels (b)–(d) in Fig. 16 shows that in the model of Fig. 15, depending on whether the thresholds can be passed back and forth, domino-like transitions in the network of phosphorylation–dephosphorylation cycles may or may not be driven by the periodic operation of the cAMP oscillator which runs in full independence from the network on which it exerts its control. Moreover, part of the cycles of the network may display repetitive domino-like transitions while other cycles located further in the network may lose them. In the models considered in earlier sections of this paper, holding a domino in the network of coupled phosphorylation–dephosphorylation cycles necessarily stopped the clock. Here, in contrast, holding a domino in one of the cycles does not affect the clock and does not prevent the occurrence of repetitive transitions in other cycles of the network located closer from the source of oscillations.

7. Discussion

The dynamics of many cellular processes depends on the operation of networks of phosphorylation–dephosphorylation cycles. A case in point is provided by the sequential activation of a variety of cyclin-dependent kinases which control the successive phases of the eukaryotic cell cycle. A decade ago Murray & Kirschner (1989) proposed to view the progression through the successive biochemical steps of the cell cycle as the falling of a row of dominoes, each step bringing the activation of the next one in the pathway. These authors pointed out that the stepwise progression along the different phases of the cell cycle could also be viewed as being driven by a continuous biochemical oscillator. Therefore, they proposed to unify the two views of the cell cycle as dominoes and clock. To clarify the link between the two modes of dynamic behavior, we have investigated a theoretical model displaying the dynamics of dominoes and clocks. As in the cell division cycle, the model is based on a network of phosphorylation–dephosphorylation reactions, but it retains a general form not directly related to the sequence of steps controlling the cell cycle dynamics. Some insights provided by the model may nevertheless bear on the dynamics of the cell cycle, as discussed below for the arrest of oscillations by protein kinase inhibitors.

We have investigated the different modes of dynamic behavior of an abstract, cyclically organized network of phosphorylation–dephosphorylation cycles (Fig. 1). In each covalent modification cycle i ($i = 1, \ldots, N$) of this *circulator* model, a protein Y_i is transformed (phosphorylated) into the form X_i. We assumed that owing to the phenomenon of zero-order ultrasensitivity, each cycle is characterized by a sharp threshold in the Y_i to X_i conversion as the ratio of maximum phosphorylation vs. dephosphorylation rates is increased (see Fig. 2). Two types of coupling between the different phosphorylation–dephosphorylation cycles were considered: a forward activation by X_{i-1} of the Y_i to X_i conversion in the next cycle in the network, and a backward activation by X_{i+2} of the X_i to Y_i conversion. The former regulation ensures that each cycle in the network is turned on by the preceding cycle: the rise in X_{i-1} will activate the transition from Y_i to X_i, and the increase in X_i will bring about the rise in X_{i+1}. To counterbalance these positive interactions, and to allow for the possibility of oscillations in the network, the second type of regulation ensures that after

a variable X_i has risen, its level is brought down after a lag by the rise in variable X_{i+2} two cycles further in the network. Thus, the rise in X_i is followed, successively, by the rise in X_{i+1} and X_{i+2}, the latter causing the decrease in X_i. We have also considered the possibility that the increase in X_{i+1} brings down the level of X_i, but found that the delay is then too short to allow for sustained oscillations. We verified that qualitatively similar results are obtained with longer delays, when assuming, for example, that the rise in X_{i+3} or X_{i+4} (for $N > 4$) brings down the level of X_i.

We first dealt with the general case in which the phosphorylation–dephosphorylation cycles of the network are linked through both forward and backward coupling (Fig. 1). In such a case, sustained oscillations are observed in a parameter domain that corresponds to the region around the threshold at which protein phosphorylation sharply increases in each cycle (Fig. 4). Each cycle in the network is then turned on sequentially in a series of domino-like transitions [Fig. 3(a)]: the rise and decay in each phosphorylated protein thus propagate along the network. The system behaves as a limit-cycle clock because this sequence of rise-and-fall transitions possesses a repetitive nature. The dominoes aspect of the oscillations is reflected by the nearly square appearance of the limit cycle [Fig. 3(b)] which is due to the abrupt nature of the on and off switching of each phosphorylated protein in the network.

Bifurcation diagrams (Figs 5 and 6) show that sustained oscillations occur in precise conditions, i.e. in a certain range of parameter values. Outside this range the network model evolves toward a stable steady state. At the borders of the oscillatory domain, because of the subcritical nature of the Hopf bifurcations, a domain exists in which a stable limit cycle coexists with a stable steady state (Fig. 5). The bifurcation diagrams confirm the importance of thresholds for the occurrence of sustained oscillations. Indeed, the latter only occur when the phenomenon of zero-order ultrasensitivity produces sufficiently sharp transitions in the steady-state levels of phosphorylated protein (Fig. 2). The degree of ultrasensitivity required to produce oscillations does not change significantly as the number of cycles in the network N increases. Besides the zero-order effect, other sources of ultrasensitivity, such as enzyme cooperativity, could also favor oscillations.

To reduce the exploration of dynamic behavior in parameter space we primarily focused on the symmetrical case where all the cycles of the network are characterized by identical kinetic parameters. We verified, however, that sustained oscillations can also occur in asymmetrical conditions (Fig. 7). In such conditions (see Section 3), particularly for $\beta > \alpha$, more complex patterns of oscillations are possible, which sometimes coexist with the simple sequential oscillations of the type shown in Fig. 3.

New modes of dynamic behavior are observed when the phosphorylation–dephosphorylation cycles are coupled through only forward or backward regulatory interactions (Fig. 11). In the former case, when each variable X_i only promotes the conversion of Y_{i+1} into X_{i+1}, bistability accompanied by hysteresis is observed over a range bounded by two critical parameter values [Fig. 12(a)]. Regardless of the number of cycles N, either all X_i are low while the forms Y_i are high, or the reverse situation obtains, depending on the initial conditions [Fig. 12(b) and (c)].

When only backward coupling is considered, i.e. when each variable X_i solely promotes the conversion of X_{i-2} into Y_{i-2}, the type of dynamic behavior depends on the number of cycles (Table 1). Thus, when N or $N/2$ are odd (as in the scheme of Fig. 13), sustained oscillations are observed for appropriate parameter values. These oscillations (Fig. 14) are similar to those obtained in the general case (Fig. 3). When $N/2$ is even, oscillations are replaced by multistability. The latter behavior is of the pitchfork type [Fig. 12(d)], with variables divided in two groups reaching either a high or a low value. Four different stable steady states can be reached in such conditions, as shown in Fig. 12(e) and (f) for the case $N = 4$. This is due to the existence of two independent subgroups containing, respectively, the coupled variables (X_1, X_3) and (X_2, X_4). Increasing N when $N/2$ is even does not increase the number of possible steady states. Thus, for $N = 8$, the network actually consists of two independent subgroups containing, respectively, the variables (X_1, X_3, X_5, X_7) and (X_2, X_4, X_6, X_8). Within each group, the four variables are coupled

TABLE 1

Modes of dynamic behavior of the network model as a function of the number of phosphorylation–dephosphorylation cycles N and of parameters α and β measuring, respectively, the strength of forward and backward coupling. The results are summarized for the fully symmetrical case in which all kinetic parameters are identical for each phosphorylation–dephosphorylation cycle. More complex situations can arise when $N > 6$ and $\alpha \neq \beta$, with $\alpha, \beta \neq 0$ (see text)

	$N = 3$	$N = 4$	$N = 5$	$N > 5$
$\alpha = 1$ $\beta = 1$	Steady state	Oscillations (Hopf)	Oscillations (Hopf)	Oscillations $\forall N$
$\alpha = 1$ $\beta = 0$	Steady state	Bistability (Hysteresis)	Bistability (Hysteresis)	Bistability $\forall N$
$\alpha = 0$ $\beta = 1$	Oscillations* (Hopf)	Four stable steady states (Pitchfork)	Oscillations (Hopf)	Four stable steady states if: $N/2$ = even number Oscillations if: N or $N/2$ = odd number

*For oscillations to occur for $N = 3$ in the case $\alpha = 0, \beta = 1$, a certain degree of asymmetry is needed. Oscillations occur, for example, for $V_{Mi} = 1$ and $V'_{Mi} = 0.7$ ($i = 1, \ldots, 3$).

in such a way that only two steady-state situations may be encountered within each group (e.g. X_1 high, X_3 low, X_5 high and X_7 low, or the reverse situation). All in all, four distinct stable steady states are possible. The evolution toward either one of these states depends on initial conditions.

Oscillations resulting from cyclically organized negative feedback interactions have been described in a number of other biological contexts. Thus, in neurobiology, regulatory interactions known as cyclic inhibition can readily produce oscillatory activity in neural networks (Kling & Szekely, 1968). More closely related to the mechanism considered here are the theoretical (Thomas *et al*., 1976; Thomas & d'Ari, 1990) and recent experimental studies (Elowitz & Leibler, 2000) showing the occurrence of oscillations due to cyclically organized negative feedback loops in genetic control systems. A final illustration is provided by the case of the stability of idiotypic networks in immunology, where forward as well as backward regulatory interactions were considered in a theoretical study (Hiernaux, 1977) which showed the possibility of sustained oscillations in antibody production when the cyclically organized idiotypic network contains an odd number of elements. That study, as well as those of genetic control circuits (Thomas *et al*., 1976; Thomas & d'Ari, 1990), also showed the possibility of multistability when the number of elements in the network is even. A similar conclusion was reached in the present model for even values of $N/2$ (see Table 1).

A further similarity between the *circulator* model of coupled phosphorylation–dephosphorylation cycles and the idiotypic and genetic control networks is that in all cases the coupling occurs via regulatory interactions rather than direct chemical transformation of one element of the network into the next element, as occurs, for example, in metabolic cycles. The possibility of oscillations in cyclical chains of chemical reactions was investigated by Hearon (1953) who showed the absence of sustained oscillations in such systems in the case of linear kinetics. The cyclical nature of some biochemical pathways does not ensure *per se* the occurrence of metabolic oscillations. Such oscillations occur only under precise conditions, in the presence of appropriate regulation of some of the enzymatic steps in the pathway. Thus, oscillations in the glycolytic pathway occur owing to the activation of the allosteric enzyme phosphofructokinase by a reaction product (Goldbeter, 1996). Oscillations can also occur in linear sequences of biochemical reactions in the presence of end-product inhibition (Tyson & Othmer, 1978).

The present study relates to theoretical studies devoted to the dynamic behavior of networks of protein modules endowed with threshold-like properties originating from zero-order ultrasensitivity in covalent modification. Previous studies stressed the possibility of performing logical operations by means of such biochemical systems (Arkin & Ross, 1994; Bray, 1995). A recent study of a large-scale model of a network of randomly connected, highly idealized kinase and phosphatase components also showed the occurrence of multiple attractors and oscillations due to negative or positive regulatory interactions (James *et al*., 1999).

The *circulator* model could be extended to the case of a cascade where X_i is itself (rather than an activator of) the kinase that catalyzes the conversion of Y_{i+1} into X_{i+1}. The latter situation was considered in a simple cascade model for the mitotic oscillator in embryonic cells (Goldbeter, 1991, 1996). In that three-variable model, thresholds due to zero-order ultrasensitivity (Fig. 2) are also required for sustained oscillations (Goldbeter & Guilmot, 1996) which originate from a negative feedback loop. There, indeed, activation of the cdc2 protein kinase (now known as cdk1) through dephosphorylation is brought about by the accumulation of cyclin B, and cdc2 kinase activates through phosphorylation an enzyme involved in cyclin proteolysis; the repetitive activation of cdc2 kinase is driven by cyclin synthesis. Here, because of the cyclical organization of the positive and/or negative feedback interactions, sustained oscillations do not rely on protein synthesis but are driven by ATP hydrolysis in each phosphorylation–dephosphorylation cycle of the network (see right panel in Fig. 1).

A key aspect of the analogy of dominoes and clocks investigated in the *circulator* model pertains to the effect of an inhibitor that would block the system in a given point by preventing the progression to the next step in the network. Thus, when assuming that an inhibitor I reduces the rate of conversion of Y_1 into X_1 (Fig. 8)—precisely as protein inhibitors reduce the activity of cyclin-dependent kinases in the cell cycle (Morgan, 1995; Sekiguchi & Hunter, 1998)—oscillations stop immediately as the system reaches a steady state; periodic behavior resumes as soon as the inhibitor is removed (Fig. 9). From a dynamical point of view, impeding the fall of the dominoes by holding one of them thus corresponds to arresting the clock by means of an inhibitor that brings the system into a stable steady state, regardless of the phase of the oscillations at which the inhibition occurs (Fig. 10). While the effect of an inhibitor generally lasts only the time during which it is present, in the case of hard excitation where a stable steady state coexists with a stable limit cycle (see Figs 4–6) the transient action of an inhibitor may suppress the oscillations in a prolonged manner. Indeed, in such conditions, when the inhibitor is removed, instead or returning to the limit cycle the system may evolve toward the stable steady state that coexists with the stable limit cycle in the domain of hard excitation [see Fig. 5(b)].

The immediate arrest of oscillations by kinase inhibitors (Fig. 9) is reminiscent of the way inhibitors of cyclin-dependent kinases block the cell in a given phase of the cell cycle. Such pause-inducing mechanisms, known as checkpoints (Hartwell & Weinert, 1989), have been included in more detailed models of the eukaryotic cell cycle (Novak *et al*., 1998; Chen *et al*., 2000). Even though the present model does not apply directly to the cell cycle, it suggests that the stepwise progression along the different phases of the cycle, temporarily halted by the transient action of inhibitors, corresponds to the dynamics of an *impeded limit-cycle oscillator* which is transiently moved into a stable steady state in the presence of such inhibitors and resumes its periodic operation as soon as they are removed. This view can be related to conclusions drawn by Aguda (1999a, b) from theoretical studies on the nature of checkpoints in the cell cycle. By analysing models involving phosphorylation–dephosphorylation cycles centered around the kinase cdc2, the phosphatase cdc25 and the kinase wee1, this author showed that the G2-M checkpoint may be associated with control of the passage through a critical parameter value corresponding to a transcritical bifurcation point beyond which a new steady state is established. One of the network models analysed here, namely the network with only forward activation (Fig. 11, left panel) resembles an abstract extension of simpler models to a ring of phosphorylation–dephosphorylation cycles, suggested by Aguda

(see Fig. 6 in Aguda, 1999a). The present analysis focused explicitly on the oscillatory dynamics and the multistability properties of such networks subjected to a variety of forward or/and backward regulatory interactions.

In the *circulator* model, the network of coupled phosphorylation–dephosphorylation cycles displays the dynamics of both dominoes and clocks. The sequence of all-or-none transitions constitutes the clock mechanism itself. Preventing any one transition from one step to the next in the sequence immediately stops the oscillations in the whole network (see Figs 9 and 10). No oscillations is lost, however, when a particular step happens to become independent of the other steps, without breaking the coupling between preceding and following steps in the sequence, as in the case illustrated in Fig. 7(b). By analysing a model based on a linear sequence of phosphorylation–dephosphorylation cycles, not able to generate oscillations by itself, we showed that oscillations can occur in such a network when it is passively coupled to an independent clock. Preventing a particular transition in the sequence can then suppress the propagation of large-amplitude oscillations through and beyond this step without affecting repetitive domino-like transitions in the preceding steps (Fig. 16). This key difference in dynamic behavior, due to the independence of the clock from the operation of the network of phosphorylation–dephosphorylation cycles, provides a diagnostic tool for distinguishing between the two situations.

Does any oscillatory system necessarily display the dynamics of dominoes? An oscillation always reflects the (generally) periodic recurrence of a sequence of steps: each element in the pathway reaches a maximum at a particular phase and brings about the transition to the next step of the oscillatory mechanism until the final step returns the system to its initial state and the cycle resumes. Not all oscillations, however, are characterized by the succession of well separated, successive steps as in the present model; such a separation is due to the existence of very sharp thresholds. In other cases [see, for example, Fig. 3(c)], periodic variations are much less abrupt as successive steps blend into each other in the course of time in a much smoother manner. The model analysed here shows that oscillatory processes in biochemistry can sometimes be viewed both as dominoes and clocks, and that a continuum of clock waveforms exists of which the fall of dominoes represents a limit.

We wish to dedicate this article to the memory of Joel Keizer. We thank the referees and N. Markadien for fruitful suggestions. This work was supported by the programme "Actions de Recherche Concertée" (ARC 94-99/180) launched by the Division of Scientific Research, Ministry of Science and Education, French Community of Belgium and by grant no. 3.4607.99 from the Fonds de la Recherche Scientifique Médicale (FRSM, Belgium).

REFERENCES

AGUDA, B. D. (1999a). Instabililities in phosphorylation–dephosphorylation cascades and cell cycle checkpoints. *Oncogene* **18,** 2846–2851.

AGUDA, B. D. (1999b). A quantitative analysis of the kinetics of the G_2 DNA damage checkpoint system. *Proc. Natl Acad. Sci. U.S.A.* **96,** 11 352–11 357.

ARKIN, A. & ROSS, J. (1994). Computational functions in biochemical reaction networks. *Biophys. J.* **67,** 560–578.

BRAY, D. (1995). Protein molecules as computational elements in living cells. *Nature* **376,** 307–312.

CHEN, K. C., CSIKASZ-NAGY, A., GYORFFY, B., VAL, J., NOVAK, B. & TYSON, J. J. (2000). Kinetic analysis of a molecular model of the budding yeast cell cycle. *Mol. Biol. Cell* **11,** 369–391.

ELOWITZ, M. B. & LEIBLER, S. (2000). A synthetic oscillatory network of transcription regulators. *Nature* **403,** 335–338.

GOLDBETER, A. (1991). A minimal cascade model for the mitotic oscillator involving cyclin and cdc2 kinase. *Proc. Natl Acad. Sci. U.S.A.* **88,** 9107–9111.

GOLDBETER, A. (1996). *Biochemical Oscillations and Cellular Rhythms: The Molecular Bases of Periodic and Chaotic Behaviour*. Cambridge: Cambridge University Press.

GOLDBETER, A., DUPONT, G. & BERRIDGE, M. J. (1990). Minimal model for signal- induced Ca^{2+} oscillations and for their frequency encoding through protein phosphorylation. *Proc. Natl Acad. Sci. U.S.A.* **87,** 1461–1465.

GOLDBETER, A. & GUILMOT, J. M. (1996). Thresholds and oscillations in enzymatic cascades. *J. Phys. Chem.* **100,** 19 174–19 181.

GOLDBETER, A. & KOSHLAND JR., D. E. (1981). An amplified sensitivity arising from covalent modification in biological systems. *Proc. Natl Acad. Sci. U.S.A.* **78,** 6840–6844.

GOLDBETER, A. & KOSHLAND, D. E. JR. (1982). Sensitivity amplification in biochemical systems. *Quart. Rev. Biophys.* **15,** 555–591.

GOLDBETER, A. & SEGEL, L. A. (1977). Unified mechanism for relay and oscillation of cyclic AMP in *Dictyostelium discoideum*. *Proc. Natl Acad. Sci. U.S.A.* **74,** 1543–1547.

HARTWELL, L. H. & WEINERT, T. A. (1989). Checkpoints: control that ensure the order of cell cycle events. *Science* **246,** 629–634.

HEARON, J. Z. (1953). The kinetics of linear systems with special reference to periodic reactions. *Bull. Math. Biophys.* **15,** 121–141.

HIERNAUX, J. (1977). Some remarks on the stability of the idiotypic network. *Immunochemistry* **14,** 733–739.

JAMES, A., SWANN, K. & RECCE, M. (1999). Cell behaviour as a dynamic attractor in the intracellular signalling system. *J. theor. Biol.* **196,** 269–288.

KLING, U. & SZEKELY, G. (1968). Simulation of rhythmic nervous activities. I. Function of networks with cyclic inhibitions. *Kybernetik* **5,** 89–103.

MARTIEL, J. L. & GOLDBETER, A. (1987). A model based on receptor desensitization for cyclic AMP signaling in *Dictyostelium* cells. *Biophys. J.* **52,** 807–828.

MORGAN, D. O. (1995). Principles of cdk regulation. *Nature* **374,** 131–134.

MURRAY, A. W. & KIRSCHNER, M. W. (1989). Dominoes and clocks: the union of two views of the cell cycle. *Science* **246,** 614–621.

NOVAK, B., CSIKASZ-NAGY, A., GYORFFY, B., CHEN, K. & TYSON, J. J. (1998). Mathematical model of the fission yeast cell cycle with checkpoint controls at the G1/S, G2/M and metaphase/anaphase transitions. *Biophys. Chem.* **72,** 185–200.

SEKIGUCHI, T. & HUNTER, T. (1998). Induction of growth arrest and cell death by overexpression of the cyclin-Cdk inhibitor p21 in hamster BHK21 cells. *Oncogene* **16,** 369–380.

THOMAS, R. & D'ARI, R. (1990). *Biological Feedback*. Boca Raton, Fl: CRC Press.

THOMAS, R., GATHOYE, A.-M. & LAMBERT, L. (1976). A complex control circuit. Regulation of immunity in temperate bacteriophages. *Eur. J. Biochem.* **71,** 211–227.

TYSON, J. J. & OTHMER, H. G. (1978). The dynamics of feedback control circuits in biochemical pathways. In: *Progress in Theoretical Biology*, (Snell, F. & Rosen, R., eds), Vol. 5, pp. 2–62. New York: Academic Press.